

N 9 3 - 2 9 6 9 8

CHARACTERIZATION OF A SPACE ORBITED INCOHERENT FIBER OPTIC BUNDLE

Stephen A. DeWalt, Edward W. Taylor

AFSC Phillips Laboratory
Directorate of Space and Missiles Technology
Kirtland AFB, NM 87117-6008
Telephone: (505) 846-4741; FAX: (505) 846-2290

ABSTRACT

The purpose of this paper is to report the results of a study performed to determine the effects of adverse space environments on a bundle of over 1800 optical fibers orbited for 69 months. Experimental results are presented on an incoherent fiber optic bundle oriented in low Earth orbit aboard the Long Duration Exposure Facility (LDEF) satellite as part of the Space Environment Effects Experiment (M0006). Measurements were performed to determine if space induced radiation effects changed the fiber bundle characteristics. Data demonstrating the success of light transmitting fibers to withstand the adverse space environment are presented.

INTRODUCTION

The M0006 experiment was implemented and managed by the Air Force Technical Applications Center (AFTAC) located at Patrick AFB, FL. One subset of the experiment consisted of an incoherent fiber optic bundle some 62 cm in length. The bundle contained approximately 1800 individual optical fibers. The M0006 and bundle location were 40° distant from the trailing edge of the LDEF. The M0006 experiment was contained within one of five experiment exposure control canisters (EECC) and remained open roughly between the period of April 21, 1984 through March 15, 1985, exposing the fiber optic bundle and other components to the space environment.

At the request of AFTAC, the Phillips Laboratory performed an investigation to determine the effects of the space environment on the fiber optic bundle in conjunction with an ongoing analysis of LDEF Exp # M0004 (Ref 1). In the next sections, the manner by which the measurements were performed and the resulting data are discussed. These measurements included investigation of the attenuation of optical signal transmission, numerical aperture and fiber spectral responses over a wide wavelength range. The measurements were performed in a sequenced manner or hierarchy in order to determine if the optical fibers experienced any space radiation induced attenuation. Thus as shown in Table 1, attenuation measurements were first performed at long wavelengths to determine the fiber attenuation without activating the photobleaching of any space radiation induced attenuation.

Thermal Parameters

Orbital temperature data for the LDEF satellite was recorded by the Thermal Measurement System (THERM) experiment P0003 (Ref 2). Post orbit thermal modeling of many positions or nodes on LDEF were matched to THERM data. Thermal modeling of representative external and internal nodes aboard the LDEF structure determined that the M0006 EECC and optical fiber bundle were exposed to wide external transient orbital temperatures. These temperatures ranged from 42.6 °C at +52° β to -32.1°C at -52° β while the EECC was opened. Here, β is the angle between the plane of the orbit of the LDEF satellite and the sun illumination vector. Temperatures of 34.6° C at +52° β and 18.1° C at -52° β were experienced while the EECC was closed.

The M0006 characterization studies were performed over a room temperature range (T_R) of 21°C \leq T_R \leq 25° C.

Measurement Techniques

Shown in Figure 1 is the substitution measurement method used to determine optical signal attenuation. The substitution method consists of injecting a known reference power level into the incoherent fiber optic bundle (IFOB) of unknown attenuation and maximizing the throughput to the detector (Ref 3). The alignment position (see Figure 1) is then keyed to allow removal of the orbited IFOB during other tests, and to allow the measurements to be repeated for accuracy. By measuring the optical power out of the IFOB and comparing to the known reference power level through the Sample fiber optic bundle (see Figure 1a) an attenuation value is obtained for the orbited IFOB. The attenuation for the IFOB can then be correlated to its total length to yield an attenuation value per unit length.

Attenuation and Spectral Measurements

The attenuation (a) measurements were performed as shown in Table 1 and carefully avoided inducing annealing of any orbital induced radiation color centers (Ref 4). The experiment configuration is shown in Figure 1. The attenuation measurements were first performed at $\lambda = 1.30 \mu\text{m}$ (a_1). This first measurement was performed to establish a baseline to which succeeding attenuation measurements could be compared. By determining the IFOB attenuation at a wavelength far removed from known photobleaching wavelengths, a measure of non-space radiation induced attenuation can be made. The measurement is next repeated at a significantly lower wavelength ($\lambda = 0.86 \mu\text{m}$). This lower wavelength is nearer to an annealing wavelength and the attenuation is again noted (a_2) (Refs 5, 6). Finally the measurement was repeated at $\lambda = 1.30 \mu\text{m}$, and all three attenuation values were then compared as shown in Table 1. The above procedure should therefore result in a *decreased* a for the repeated $\lambda = 1.30 \mu\text{m}$ measurement if any laboratory induced photobleaching of space induced radiation damage occurred at $0.86 \mu\text{m}$.

As can be seen in Table 1, a *decrease* of $a_3 - a_1 = -0.20 \text{ dB/m}$ was measured at $1.30 \mu\text{m}$, following the $0.86 \mu\text{m}$ measurement, which could indicate that space radiation induced attenuation occurred. However, this measured a is not thought to be significant since the accuracy of the substitution measurement method as shown in Figure 1 was determined to be $\pm 8.1 \%$ or $\pm 0.42 \text{ dB/m}$ (limitations of the detector system and reflections induced by the interface of the sample fiber optic bundle and IFOB) at $\lambda = 1.30 \mu\text{m}$.

Next, a measurement of increased optical power ($\leq 5 \mu\text{W}$) at the lower $0.86 \mu\text{m}$ wavelength was performed and again was followed by a measurement at $1.30 \mu\text{m}$ of an optical power of less than $1 \mu\text{W}$. This procedure should result in a *decreased* a for both repeated wavelengths if any laboratory photobleaching of space induced attenuation occurred. In this instance a *decrease* of $a_4 - a_2 = -0.35 \text{ dB/m}$ was measured at $0.86 \mu\text{m}$ and an *increase* was seen in a_5 at $1.30 \mu\text{m}$. Thus, it was clear that no systematic photobleaching was occurring since one would expect the attenuation a_5 to mimic the a_3 measurement or *decrease* from the a_3 value. Again, the measured attenuation difference ($a_4 - a_2$) at $0.86 \mu\text{m}$ is not thought to be significant since the accuracy of the substitution method was determined to be $\pm 0.46 \text{ dB/m}$ at $0.86 \mu\text{m}$ or $\pm 8.1 \%$ of the a_2 measurement. Furthermore, the radiation dose received by the space orbited bundle was 210.2 rads (LiF) as measured by thermoluminescent dosimeters (TLDs) on board the experiment which is a very low dose and was not expected to induce radiation damage in the IFOB. These TLDs were shielded by aluminum which provided an effective mass thickness of 0.43 g/cm^2 while the EECC was opened and 10 g/cm^2 while EECC was closed (ref. 7,8).

Following measurement sequence #5 in Table 1, further attempts to determine space radiation induced attenuation were accomplished by measuring the IFOB's spectral irradiance response over a wide wavelength range (i.e. $0.40 \mu\text{m} \leq \lambda \leq 0.70 \mu\text{m}$). This intense and low wavelength scan would be expected to photobleach any shallow color centers sites, thus resulting in *lower* a values at $\lambda = 1.30 \mu\text{m}$ and $\lambda = 0.86 \mu\text{m}$ then were previously measured.

The scan was performed using a 100 W mercury arc lamp with a 0.5% current ripple peak to peak (0.17% RMS) and a monochromator-data acquisition system with a system reliability of $\pm 3 \%$ percent in spectral irradiance (refer to Figure 2). A spectral irradiance reference point was established at $0.65 \mu\text{m}$ of $3.43 \mu\text{W cm}^{-2} \text{ nm}^{-1} \pm 0.1 \mu\text{W cm}^{-2} \text{ nm}^{-1}$ to assure continuity for other spectrophotometry scans.

Partial scans were performed ranging from 0.40 μm through 0.70 μm , and from 0.70 μm through 1.10 μm . In between these two spectrophotometer scans and after the second spectrophotometer scan of 0.70 μm through 1.10 μm , a comparison of results to detect photobleaching was again performed on the fiber bundles at 1.30 μm and 0.86 μm at an optical power of less than 1 μW .

As may be observed in Table 1, attenuation measurements were performed following the first spectral scan (measurement sequences #6 and #7). It is apparent in the measurement sequences #6 and #7 that both attenuation measurements $a_6 - a_1 = -0.27 \text{ dB/m}$ at 1.30 μm and $a_7 - a_2 = -0.25 \text{ dB/m}$ at 0.86 μm were lower. However, one may attribute both decreases in attenuation to their respective inherent measurement uncertainties of $\pm 0.42 \text{ dB/m}$ at $\lambda = 1.30 \mu\text{m}$ and $\pm 0.46 \text{ dB/m}$ at $\lambda = 0.86 \mu\text{m}$, and hence are not perceived to be significant. Again, the attenuation differences measured were not significant for the orbited fibers, indicating that no permanent degradation resulted due to the space exposure. Nor did the spectral scans of the control and orbited fibers show any significant deviation in absorption bands or transmission differences throughout the spectral range of 0.60 μm through 1.00 μm as may be viewed in Figure 3. One can again conclude photobleaching was not a factor in any of our measurements and is readily apparent in the final attenuation measurement sequences #8 and #9 of Table 1 (i.e. $a_8 - a_1 = -0.17 \text{ dB/m}$ at 1.30 μm and $a_9 - a_2 = -0.28 \text{ dB/m}$ at 0.86 μm) which are well within the measurement accuracies.

Numerical Aperture

To further correlate the orbited and control IFOBs, a measurement of numerical aperture (NA) was performed under far field conditions.

The far field measurement was made by using a Fourier transforming and relay lens system (Ref 9). The acceptance angles were determined to be $62.8^\circ \pm 2.5^\circ$ for the control bundle resulting in a numerical aperture of 0.52 ± 0.02 . The orbited bundle measurements resulted in an acceptance angle of $64.7^\circ \pm 2.5^\circ$ and a numerical aperture of 0.54 ± 0.02 .

Since previous records of the composition of the IFOB were incomplete, these measurements and comparisons were crucial. Through a collaborative effort with the manufacturer, several possible optical glass fiber types were identified. The exact optical glass fiber type was identified by comparing the experimentally determined far field numerical aperture to a list of possible types supplied by the manufacture.

Digitized Mapping of End Surfaces of the IFOBs

The cabled optical fiber bundle was protected during its orbital space exposure except for the very ends of the 61.7 cm fiber lengths. These flattened ends appeared to have been cleaved and polished before they were placed in the M0006 experimental tray. While no analysis could provide information on the historical preparation of the optical fiber end conditions prior to launch, a qualitative examination of the condition of the optical fiber ends was accomplished. A comparison of both the control and orbited fiber bundle ends revealed only slight variations. The control bundle showed, on one end, that roughly 20% of the individual fibers had been chipped. This damage may have been caused during the storage of the control bundle. In contrast, the space orbited bundle showed very pristine polished optical fibers, devoid of any visible damage.

Digitized mapping of both end surfaces of each fiber bundle was accomplished by using the infrared microscope-camera arrangement of Figure 4. An individual fiber count was possible by radially sectioning the mapped bundle surface into sixteen 22.5° sections (refer to Figure 5). Some $1,862 \pm 16$ fiber waveguides were measured within the control bundle and $1,838 \pm 16$ fiber waveguides were measured within the space orbited bundle. It is estimated that an error of 1 fiber waveguide per 22.5° section was inherent in the measurement, and hence a total error of ± 16 fiber waveguides was measured for both control and space orbited bundles.

The individual optical fibers were measured to have a core diameter of $60 \mu\text{m} \pm 5 \mu\text{m}$. The cladding thickness surrounding the core was measured to be $75 \mu\text{m} \pm 5 \mu\text{m}$.

Mapping was necessary to positively identify that the control bundle provided was of the same manufactured lot as that of the orbited bundle. This positive identification also allowed traceability of the

control sample to the material composition of the optical fibers. Using this identification process, correlations of the control and orbited fiber samples could be made with similar samples of fiber provided by the manufacturer of the fiber bundles.

Final Spectrophotometry Measurements

During the hierarchy of attenuation measurements a total of two scans were performed on the control and space orbited bundles (refer to Table 1). These scans revealed no significant deviations of spectral irradiance levels over the range of 0.60 μm to 1.00 μm in either the control or the flight bundle scans. Following the digitized mapping and far field measurements a final spectrophotometry scan was performed. This final scan repeated the previous results and again supported our conclusion that the space orbited fiber optic bundle did not experience any permanent radiation induced attenuation over the wavelength range of 0.60 μm to 1.00 μm (refer to Table 1 and Figure 6).

Attenuation Measurements by the Cutback Technique

While the attenuation measurements performed in Table 1 were made by substitution techniques which are non-destructive and could be repeated many times, this is not the case involved when using the cutback technique for measuring attenuation. Generally, the cutback technique is associated with single fibers, but in the following measurements the technique was applied to a fiber bundle. A final cutback attenuation measurement was executed on both bundles after all previous measurements had been completed. This test was done in order to further verify the control and orbited bundle attenuations previously measured in the substitution method. By cutting back the specimens some three times to result in varying fiber lengths, different signal attenuations are measured through smaller increments of fiber.

However, as expected, the attenuation measurements for the cutback method were lower than those obtained by the substitution method. The reason for this is that only random mating of the sample and orbited fibers (see Figure 1b) within the bundles is accomplished with the latter technique. The sample and orbited fibers of approximately 1,800 fibers in one bundle with $1,838 \pm 16$ fibers in the second bundle is very lossy. In contrast, the cutback technique as applied here involves the complete illumination and constant injection of light at one end of the bundle while at the opposite end the measurements and cuts on the bundle are administered. A large difference (i.e. at $\lambda = 0.86 \mu\text{m}$ substitution attenuation averaged minus cutback attenuation resulted in 2.6 dB/m) may be attributed to both the random coupling and the control and space orbited bundle's special fiber end preparation. The control and orbited fibers were equipped with an off-axis or canted polished surface. This canted surface was polished off on both ends of each bundle after the substitution attenuation measurements and before the cutback attenuation measurements were performed. The fiber ends were polished for ease of completion of the cutback attenuation measurements.

Due to the known accuracy of the cutback method (accuracies can be made to less than ± 0.01 dB) for determining intrinsic fiber transmission losses, the cutback attenuation data was accepted as the most accurate (Ref 10,11). For the control bundle at the wavelength 0.86 μm the attenuation was measured to be a_c (Control Bundle) = $2.77 \text{ dB/m} \pm 0.14 \text{ dB/m}$, and the orbited bundle was measured to be $a_o = 2.85 \text{ dB/m} \pm 0.14 \text{ dB/m}$. Table 2 compares the results of the space orbited and control fiber bundle measurements using these two methods and lists other observed and measured parameters. Thus, the intrinsic attenuation between the control and space orbited fiber bundles was $a_o - a_c = 0.08 \text{ dB}$, or well within the measurement accuracy of $\pm 0.14 \text{ dB/m}$.

CONCLUSION

This study successfully identified and characterized a fiber optic bundle composed of $1,838 \pm 16$ individual fibers orbited aboard the LDEF satellite. Quantification of the fiber bundle parameters included numerical aperture, intrinsic attenuation, and fiber count. A determination of the fiber bundle's physical condition was also accomplished. A strict hierarchy of measurement procedures was invoked to determine the existence of any space radiation induced attenuation. Due to the extremely short length of the optical waveguides involved, measurement accuracies were limited to $a = \pm 0.14 \text{ dB/m}$. No photobleaching of suspected permanent space induced radiation damage was observed for $0.60 \mu\text{m} \leq \lambda \leq 1.0 \mu\text{m}$ and $\lambda = 1.30 \mu\text{m}$. The analysis of this optical fiber bundle is unique since the data benchmarks the only known incoherent optical fiber bundle orbited for 69 months in low Earth orbit.

REFERENCES

- [1] Taylor E. W., et. al: Preliminary Analyses of WL Experiment #701, Space Environment Effects On Operating Fiber Optic Systems, *LDEF - 69 Months in Space - First Post Retrieval Symposium*, Report No. NASA CP-3134.
- [2] Berrios W. M.; Sampair T. R.: Long Duration Exposure Facility Post-Flight Thermal Analysis; Calculated Flight Temperature Data Package - Preliminary, Vol. 2, pp. E-21, *NASA/LaRC MS 434*, Hampton VA 23665-5225.
- [3] Fiber Optic Test Procedure - 171 (FOTP-171), "Attenuation by Substitution Measurement for Short Length Multimode Graded Index and Single Mode Optical Fiber Cable Assemblies," EIA/TIA - 455-53A-90, *Electronic Industries Association (EIA)*, 2001 Pennsylvania Avenue, Washington D.C. 20006, (202) 457-4900.
- [4] Robert, N.; Schwartz, G.; Blair, R.; Tangunan, G. L.: Radiation Damage of Germanium-Doped Silica Glasses: Spectral Simplification by Photo and Thermal Bleaching, Spectral Identification and Microwave Characteristics, *Jour. App. Phys.*, Vol. 59, No 9, 15 April 1986, pp. 30-36.
- [5] Schulman, J. H.; Compton, W. D.: Experimental Methods in Color Center Research, *Color Centers in Solids*, MacMillan Company, 1962, pp.32-49.
- [6] Allard, F. C.: Optical Fibers, Fiber Optic Test Methods, *Fiber Optics Handbook for Engineers and Scientists*, McGraw-Hill, 1990, pp. 1.25-1.32, 4.42-4.52.
- [7] Chang, J.; Kantorcik, T.; Stauber, M.: Results of M0006 Dosimeter Readings, Presented to LDEF Ionizing Radiation SIG Meeting, NASA/MSFC, Orlando FL, 25 Jan 91.
- [8] Chang, J.; Giongano, D.; Kantorcik, T.; Stauber, M.; Snead, L.: Thermoluminescent Dosimetry for LDEF Experiment M0006, (To be published in LDEF Proceedings.)
- [9] Fiber Optic Test Procedure - 47 (FOTP-47), "Output Farfield Radiation Pattern Measurements", EIA/TIA - 455 - 47A, *Electronic Industries Association (EIA)*, 2001 Pennsylvania Avenue, Washington D.C. 20006, (202) 457-4900.
- [10] Fiber Optic Test Procedure - 78 (FOTP-78), "Spectral Attenuation Cutback Measurement for Optical Fibers", EIA/TIA 455-78A-90, *Electronic Industries Association (EIA)*, 2001 Pennsylvania Avenue, Washington D.C. 20006, (202) 457-4900.
- [11] Allard, F. C.: Fiber Optic Test Methods, pp. 4.8-4.9, 4.12, 4.14.

LIST OF FIGURES AND TABLES

Table 1: Hierarchy of Measurements.

Table 2: Fiber Optic Bundle Parameters.

Figure 1: Attenuation Experiment Appartus.

Figure 2: Spectrophotometry Appartus.

Figure 3: Spectrophotometry Scan I and II.

Figure 4: Bundle End Examination Appartus.

Figure 5: Close-up of Bundle End.

Figure 6: Spectrophotometry Scan III.

Table 1 Hierarchy of Attenuation Measurements					
Measurement Sequence	Measurement Performed	Wavelength (μm)	Optical Power (μW)	Control Bundle (dB/m)	Space Orbited Bundle (dB/m)
1	Attenuation	1.3	< 1	$\alpha_1 = 5.14$	4.92
2	"	0.86	< 1	$\alpha_2 = 5.97$	5.63
3	"	1.3	< 1	$\alpha_3 = 5.20$	4.72
4	"	0.86	≤ 5	$\alpha_4 = 5.42$	5.28
5	"	1.3	< 1	$\alpha_5 = 5.35$	4.96
	Spectrophotometry Scan I (Spectral Irradiance (SI) W/cm ² ·nm ⁻¹) 3.3e-6 ≤ SI ≤ 5.4e-5	0.4 ≤ λ ≤ 0.7	-----	-----	-----
6	Attenuation	1.3	< 1	$\alpha_6 = 5.27$	4.65
7	"	0.86	< 1	$\alpha_7 = 5.80$	5.38
	Spectrophotometry Scan II 4.0e-6 ≤ SI ≤ 1.6e-5	0.7 ≤ λ ≤ 1.1	-----	-----	-----
8	Attenuation	1.3	< 1	$\alpha_8 = 5.41$	4.75
9	"	0.86	< 1	$\alpha_9 = 5.66$	5.35

Table 1 - The measurements are sequentially listed as they were performed. The Substitution measurement technique was used on all attenuation measurements. It is evident from the data that no photobleaching was observed in the Space Orbited fibers. The variance in attenuation at 1.30 μm for both Control and Space Orbited Bundles is ± 0.01 dB/m and ± 0.02 dB/m, respectively. At 0.86 μm the variance is ± 0.05 dB/m for the Control Bundle and ± 0.02 dB/m for the Space Orbited Bundle.

Table 2 Fiber Optic Bundle Parameters		
<u>CABLE</u>	<u>CONTROL BUNDLE</u>	<u>SPACE ORBITED BUNDLE</u>
Material	PVC	PVC
Color	Black	Black
Length	63.5 cm	61.7 cm
Diameter	3.2 mm	3.2 mm
Fiber Quantity	1862 ± 16	1838 ± 16
Condition - March 1990 ₁	Excellent	Excellent
<u>FIBERS</u>		
Core Material	Flint Glass (Predominately Silica and Lead)	
Clad Material	Alkaline Resistant Glass (Soda, Lime and Silicate)	
Core Diameter	60 μm ± 5 μm	
Clad Diameter	75 μm ± 5 μm	
Operational Wavelength ₂	Visible and Infrared	
<u>ATTENTION VALUES</u>		
Cutback Method	2.77 dB/m ± 0.14 dB/m	2.85 dB/m ± 0.14 dB/m
Manufacturer	1.20 dB/m ± 0.10 dB/m	1.20 dB/m ± 0.10 dB/m
<u>FOOTNOTES</u>		
1) Bundles are in four pieces as a result of Cutback Method measurements.		
2) Tested at 400 nm through 1100 nm and, 1300 nm.		

Table 2 - Known and observed incoherent fiber optic bundle characterizations.

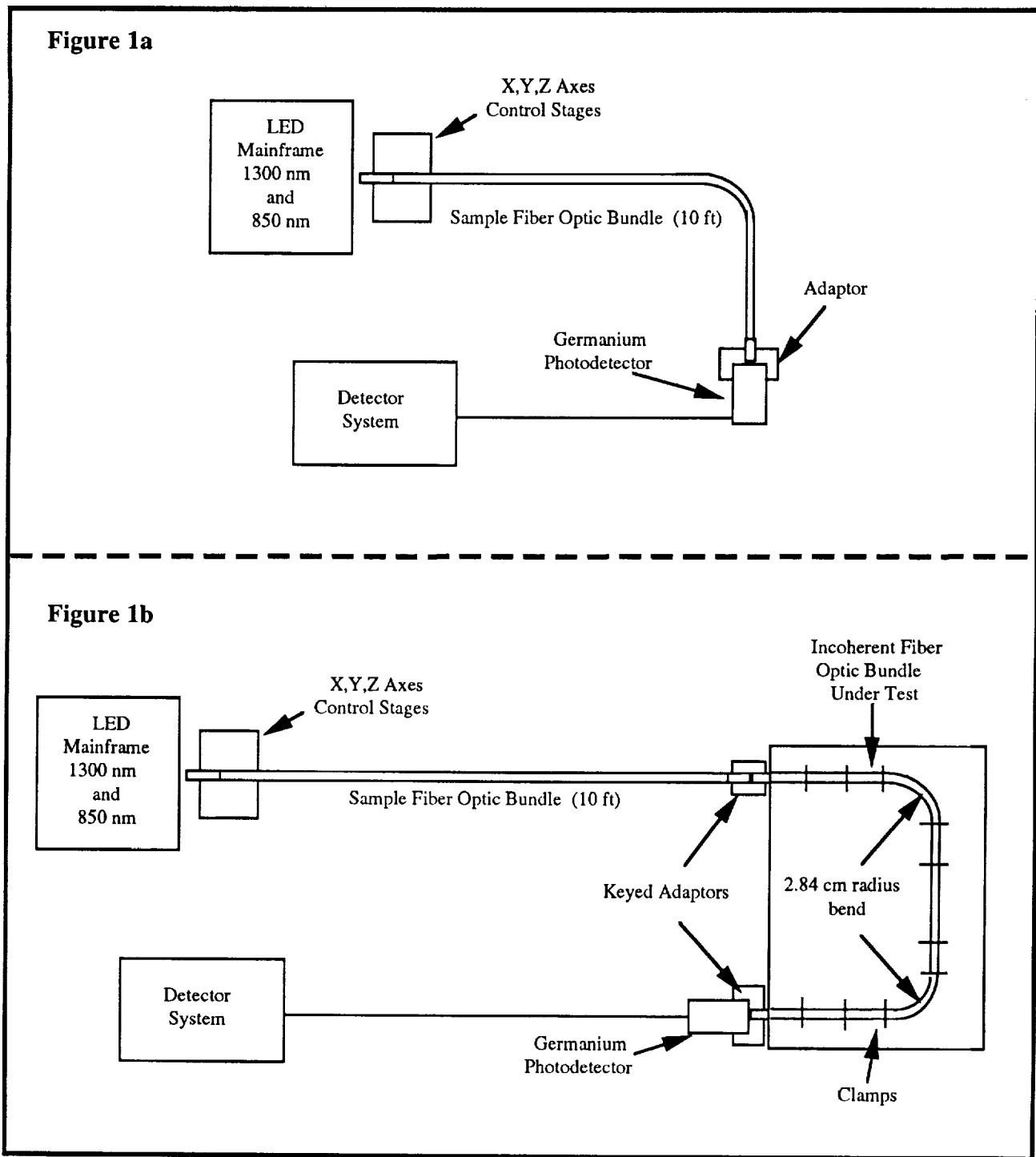


Figure 1 - Measurement of attenuation by the substitution method is shown above. In Figure 1a, a reference power measurement is established by uniformly injecting light into the Sample fiber optic bundle and detecting the power at the Photodetector. In Figure 1b a second attenuation measure is performed and in theory, the added attenuation is attributed to the Incoherent Fiber Optic Bundle Under Test. The Keyed Adaptors in Figure 1b are to insure consistency of measurement technique.

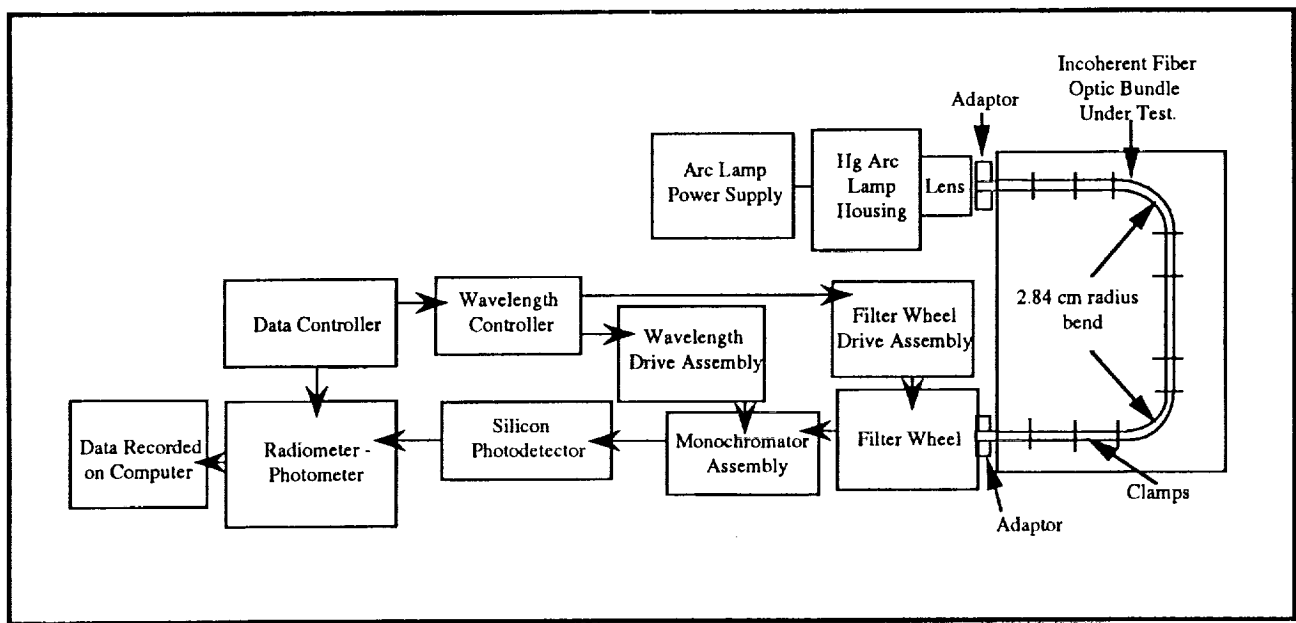


Figure 2. Spectrophotometry equipment to detect α and photobleaching is shown. A total of three spectrophotometry scans were performed on both the control and space orbited bundles. The Data Controller initiated the scans. Arrows connecting equipment represent logic flow.

Spectrophotometry Scans I and II

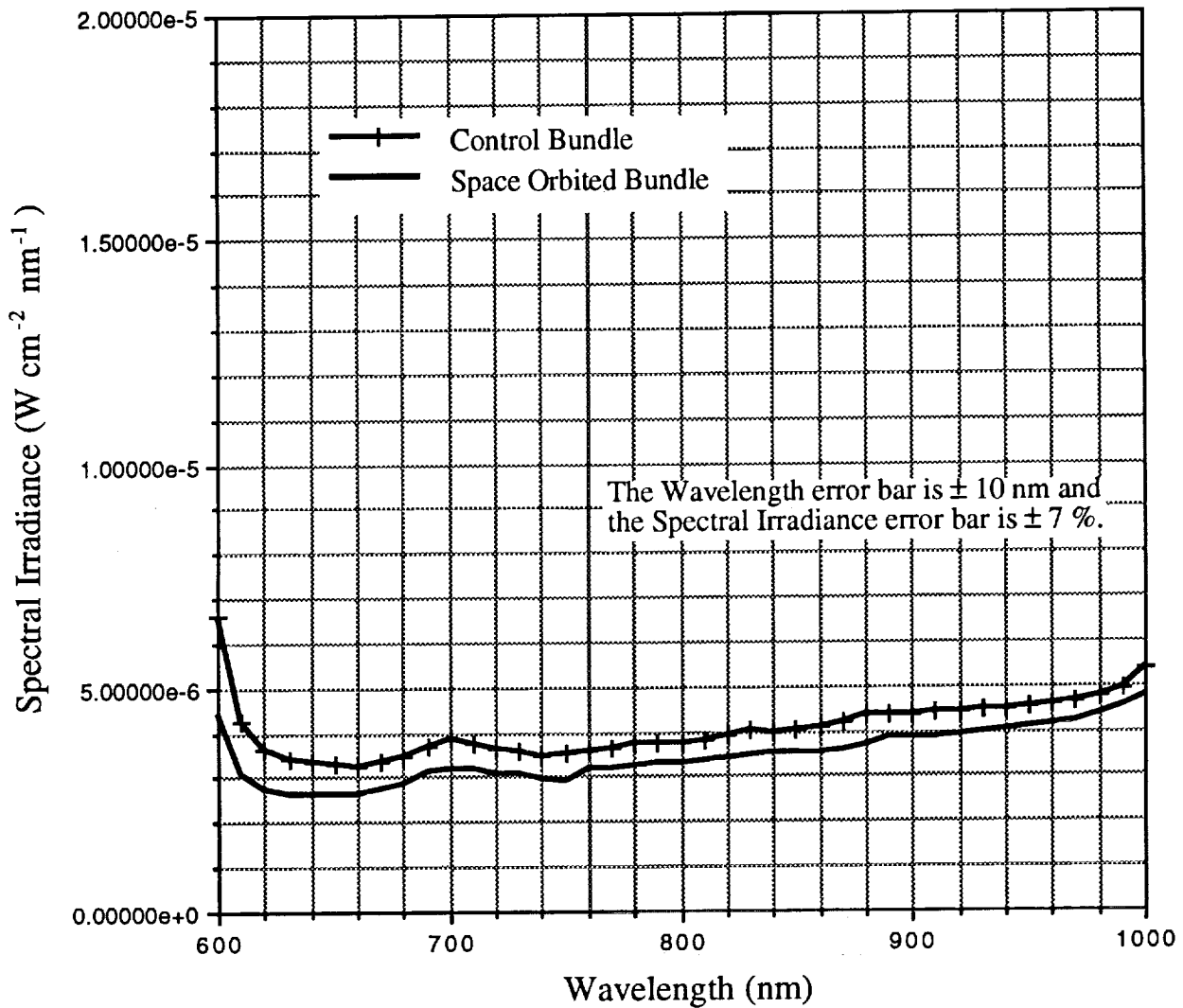


Figure 3 - The Spectrophotometry Scans I and II have been combined to reveal no significant signal transmission differences in the Control to Space Orbited fiber optic bundle comparison.

Note: Due to fluctuations in the spectrophotometry system no conclusions could be drawn over the ranges 400nm to 600nm and 1000nm to 1100nm. This fluctuation was caused by a non-synchronization of monochromator's settling times and data acquisition system's data transfer timing.

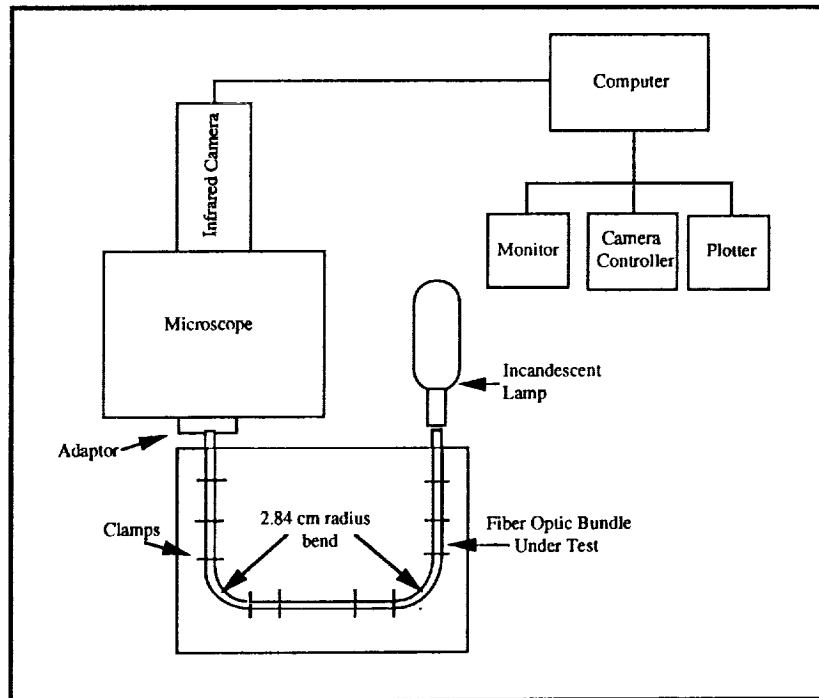


Figure 4 - An individual fiber identification was performed on both bundles with the configuration shown. The Incandescent Lamp was positioned to uniformly illuminate the Fiber Optic Bundle Under Test.

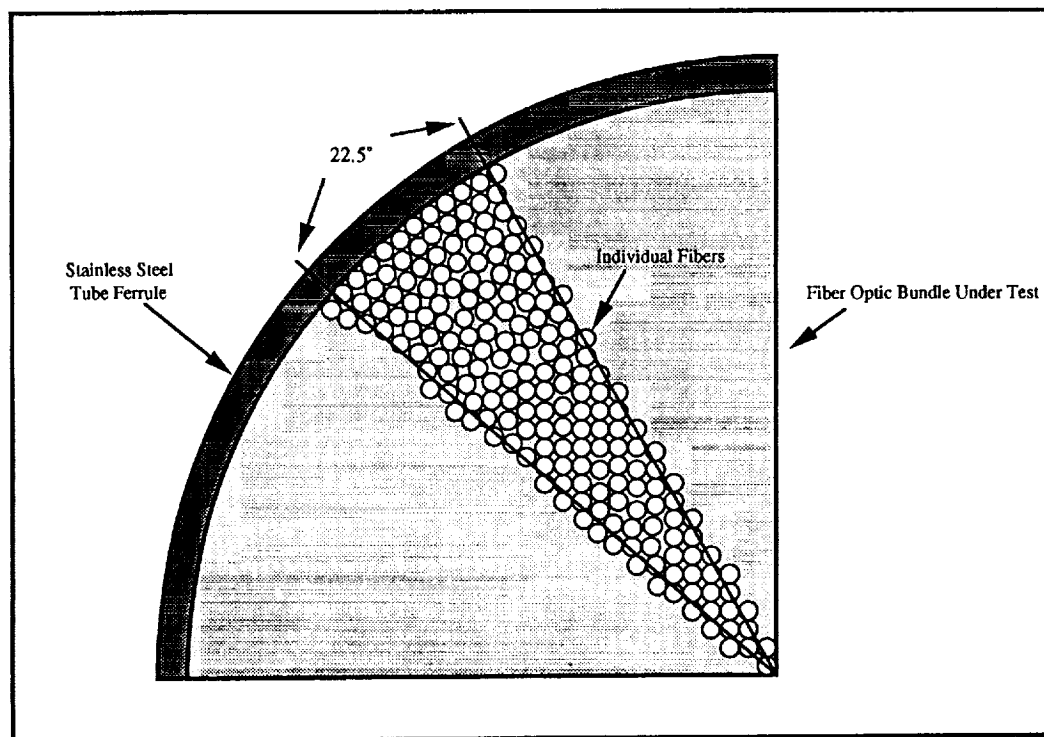


Figure 5 - An end quarter section view of the fiber optic bundle is shown. A total fiber count was obtained by sectioning the Fiber Optic Bundle Under Test into a 22.5° section as shown. Only the portion of the Individual Fibers which laid in the 22.5° section was counted. The number of Individual Fibers was then extrapolated to estimate the number of fibers in the Space Orbited and Contol bundles.

Spectrophotometry Scan III

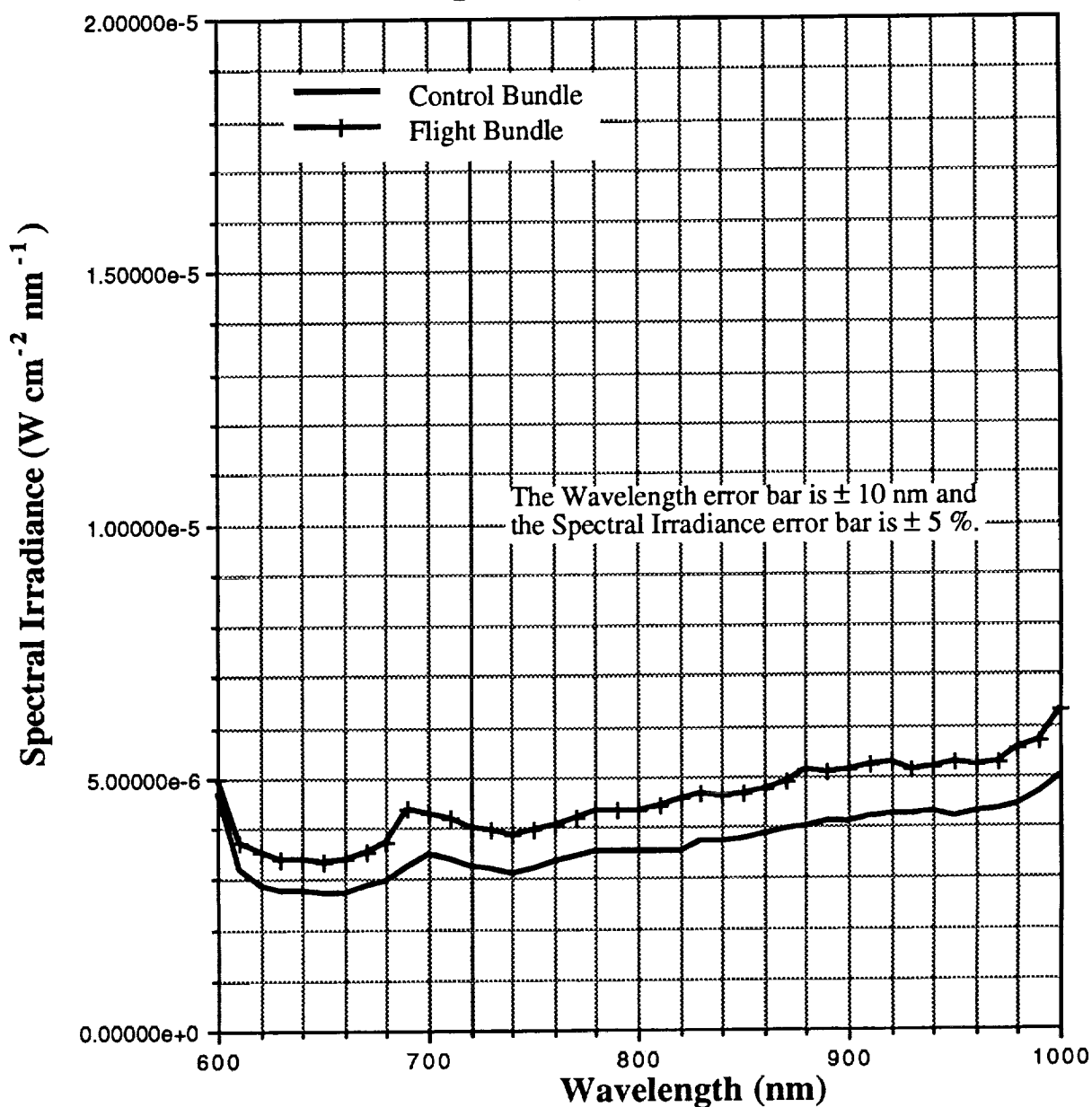


Figure 6 - The final spectrophotometry scan reveals little deviation between the Control and Space Orbited Bundles within the 600 nm to 1000 nm region.

Note: Due to fluctuations in the spectrophotometry systems no conclusions could be drawn over the ranges 400 nm to 600 nm and 1000 nm to 1100 nm. This fluctuation was caused by a non-synchronization of the monochromator's settling times and data acquisition system's data transfer timing.

1. The first part of the document discusses the importance of maintaining accurate records of all transactions and activities. It emphasizes that this is essential for ensuring transparency and accountability in the organization's operations.

2. The second part of the document outlines the various methods and tools used to collect and analyze data. It highlights the need for consistent and reliable data collection processes to support effective decision-making.

3. The third part of the document focuses on the role of technology in modern data management. It discusses how advanced software solutions can streamline data collection, storage, and analysis, leading to more efficient and accurate results.

4. The fourth part of the document addresses the challenges associated with data security and privacy. It provides guidance on implementing robust security measures to protect sensitive information from unauthorized access and breaches.

5. The fifth part of the document discusses the importance of data quality and integrity. It outlines strategies for identifying and correcting errors in data collection and processing to ensure the reliability of the information used for analysis.

6. The sixth part of the document explores the various applications of data analysis in different industries. It provides examples of how data insights can be used to optimize performance, identify trends, and make strategic decisions.

7. The seventh part of the document discusses the ethical considerations surrounding data collection and use. It emphasizes the need for transparency, informed consent, and responsible data handling practices to protect individual rights and privacy.

8. The eighth part of the document provides a summary of the key points discussed throughout the document. It reiterates the importance of data in driving organizational success and the need for a comprehensive data management strategy.

9. The final part of the document offers concluding thoughts and recommendations for future research and practice. It encourages ongoing learning and innovation in the field of data management to stay ahead of the curve in a rapidly changing digital landscape.